VOL. 12, NO. 11, JUNE 2017 ISSN 1819-6608
ARPN Journal of Engineering and Applied Sciences

www.arpnjournals.com

THE INFLUENCE OF HIGH FREQUENCY SYSTEM OF STANDING WAVE ELECTRON LINEAR ACCELERATOR ON BEAMOUTPUT PROPERTIES

Vladimir Kuz'mich Shilov, Aleksandr Nikolaevich Filatov and Aleksandr Evgen'evich Novozhilov
National Research Nuclear University MEPhI (Moscow Engineering Physics Institute) Kashirskoye Shosse, Moscow, Russian Federation
E-Mail: fila-tov@bk.ru

ABSTRACT

This article discusses high-frequency systems of standing wave linear electron accelerator. One of the drawbacks of standing wave accelerators is extended transient process in high-Q resonator sections, which leads to insufficient beam energy at initial stage of high frequency pulse and occurrence of medium energy spread of clusters. This spread can be eliminated by power supply of accelerator sections and delay of injection pulse with regard to the pulse of high frequency field. This enables fine tuning of high-frequency energy supplied to accelerating resonator sections upon simultaneous variation of time constant of transient process of electric fields setup in sections. In these systems complete decoupling of generator from high-Q accelerating sections is achieved, the influence of current load by accelerating sections decreases, and beam output properties are improved.

Keywords: high frequency supply, accelerator, magnetron, spectrum analyzer, Waveguide Bridge, attenuator, phase invertor, dissipative loading, transient process.

1. INTRODUCTION

Standing wave electron linear accelerators (linac) in some cases are more compact and efficient in comparison with running wave linac [1]. As a rule, accelerating system of such facilities is comprised of contoured cavity resonators of biperiodic slow wave structures (BSS) of various types [2]. High frequency (HF) power of accelerating sections in such linacs is supplied by magnetron or klystron amplifier and generator decoupling from high-Q accelerating resonators are performed by ferrite valves, circulators or HF bridges.

Power supply of linac accelerating sections from magnetron via Waveguide Bridge in terms of efficiency, dimensions and maintainability, cost of main and auxiliary equipment, is preferred in comparison with other power supply types [3]. In addition, with appropriate selection of bridge properties it is possible to stabilize magnetron frequency more than by an order of magnitude.

Output properties of standing wave accelerators are strongly influenced by extended transient process of GF field setup in accelerating resonator sections with high value of basic Q-factor.

It is known that accelerating resonator section can be presented in the form of resonant circuit [4], hence, accelerating electric field in BSS increases according to the following equation:

$$E(t) = E_0\left[1 - e^{-\frac{\omega t(1+\chi)}{2Q_0}}\right]. \quad (1)$$

Transient process leads to insufficient beam energy at initial stage of HF pulse and occurrence of medium energy spread of clusters [5]. This can be eliminated by delay of injection pulse with regard to the pulse of high frequency pulse. This issue was studied in [6] with regard to standing wave electron linear accelerators (linac). It was found that in order to minimize energy scatter at accelerator output it is required to apply the following delay in injection pulse with regard to HF pulse:

$$\tau_{1opt} = \frac{Q_0}{(1+\chi)\pi f} ln\frac{1}{\xi},$$

where где$\xi = I_0\sqrt{\frac{Z_{eff}l}{4\chi P_0}}$, I_0 is the average current per pulse, Q_0 is the resonator Q-factor, χ is the coupling coefficient.

The delay of injection pulse was experimentally achieved on two-sectional standing wave linac. In order to provide valid measurements of energy spectra at output the beam diagnostics was studied at first in details, since the standing wave linacs on the basis of BSS are characterized by intensive radial motion of particles. The measurements were performed by magnetic spectrum analyzer.

Axial path of electron beam was adjusted after measurements of actual topography of magnetic field using measuring coil. Accurate calculation of electron motion in inter-pole space and on magnet ends with accounting for actual distribution of magnetic induction was based on solution of the differential equations:

$$\begin{aligned}\ddot{\xi}_x &= \frac{1}{\gamma}\left(\dot{\xi}_y H_z - \dot{\xi}_z H_y\right),\\ \ddot{\xi}_y &= \frac{1}{\gamma}\left(\dot{\xi}_z H_x - \dot{\xi}_x H_z\right),\\ \ddot{\xi}_z &= \frac{1}{\gamma}\left(\dot{\xi}_x H_y - \dot{\xi}_y H_x\right),\end{aligned} \quad (2)$$

where $\gamma = \left(1 - \dot{\xi}_x^{\,2} - \dot{\xi}_y^{\,2} - \dot{\xi}_z^{\,2}\right)^{-\frac{1}{2}}$; $\xi_x = \frac{x}{\lambda}$; $\xi_y = \frac{y}{\lambda}$; $\xi_z = \frac{z}{\lambda}$; x, y, zare the Cartesian coordinates; $\lambda = 1cm$ is the

scale factor; $H_i = \frac{e\lambda H_{0i} Z_0}{m_0 c^2}$, $i = x, y, z$; H_{0i} are the values of respective components of magnetic field intensity. The dot means differentiation with respect to the reduced parameter $\tau = ct/\lambda$.

Adjustment of main path shape, angle of entry and exit of electrons into magnet inter-pole region, configuration of vacuum chamber and positions of collimators was performed for nominal value of electron output energy $5.5MeV$.

Using the measured value of magnetic induction B as a function of current in magnet winding and known equation $\beta(W + m_0c^2) = 300BR$, where β, W, R are the relative velocity, kinetic energy, and electron motion radius, respectively, it is possible to obtain kinetic energy of electrons transmitted via spectrometer as a function of winding current [7].

2. EXPERIMENTAL

The spectra were measured as follows. Faraday cups were installed on both outputs of analyzer vacuum chamber. Upon direct beam passage and at the first stage of measurements the signals were indicated by microammeters. Semiautomatic operation was maintained by specialized tools. Errors of energy measurement using magnetic spectrometer are determined by several reasons. Firstly, it is the measurement error of magnetic induction in working region by Hall sensor equaling to $\pm$1.5%. In addition, there is the error related with deviation of normal to sensor surface from direction of magnetic induction vector, actually it is not higher than $\pm$0.5%. The gap width of the collimator in the side arm of vacuum chamber is $4mm$, which at the radius of axial path of electron motion of 93 mm results in the error of energy measurement of $\pm$ 2.2%. The contributions to measurement errors are made also by instability of power sources and by measurement errors of winding current. Cumulative error of spectrum analyzer for point beam with zero divergence amounted to $\pm$3.3%.

In the course of measurements on the accelerator the analyzer input was collimated by two copper diaphragms with the hole diameter of $10mm$ at the distance of$200mm$. It should be mentioned that low displacements of beam at the first collimator and low angle variations of entry into the analyzer resulted in additional uncertainty of energy, which is equivalent to increased width of the analyzer entry gap. Measurements by sensor of partial absorptions with aluminum absorbers with the widths of 0.416, 0.983 и $1.789 g/cm^2$ installed on the analyzer output at constant currents of magnet demonstrated that scatter in the measured transmission coefficient depends on variation of HF energy, magnetron frequency, and current load on sections. As a consequence, cumulative error of energy measurement amounted to $\pm$ 5%.

The measurement accuracy was improved by higher level collimation of accelerated beam, which leads to sharp decrease in intensity at spectrometer output and creates difficulties of recording of small currents. In addition, higher level collimation of beam prevents usage of complete accelerated current at deactivated magnetic field.

3. RESULTS AND DISCUSSIONS

Figure-1a illustrates variations of spectral properties as a function of HF generator power at section input. The width of energy distribution of electrons at half-height with regard to intensity varies from 15% to 23%, which can be attributed mainly to transient processes in resonator sections.

Increase in spectrum by 8% at half-height is possible наupon increase in magnetron frequency with regard to medium resonant frequency of section as illustrated in Figure-1b. This effect is attributed to better phase sequence of clusters with regard to accelerating field in the second section with varied eigen frequencies of sections. This is evidenced by increase in active current loading of the second section, whereas the loading of the first section remains the same.

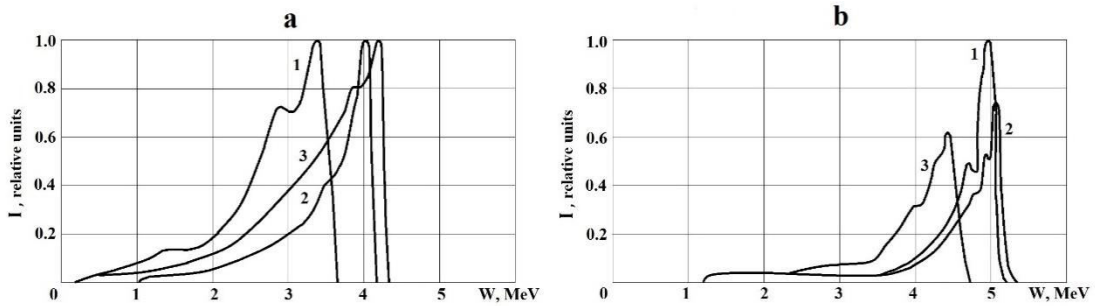

Figure-1. Energy spectra at the output of two-section accelerator: a) upon variation of generator power and beam pulse current $I_p = 40$mA: $1 - P = 1$MW, $2 - P = 1{,}2$MW, $3 - 1.3$MW; b) upon variation of generator power and beam pulse current $I_p = 15$mA: $1 - f_0$, 2 - $(f_0 - 0.15\text{MHz})$, $3 - (f_0 + 0.15)$MHz.

Figure-2 illustrates the beam energy spectra at accelerator output upon delay in injection pulse with regard to HF pulse for $P_0 = 1.5MW$ и $I_0 = 50mA$ ($\xi = 0.1$), which is close to nominal values.

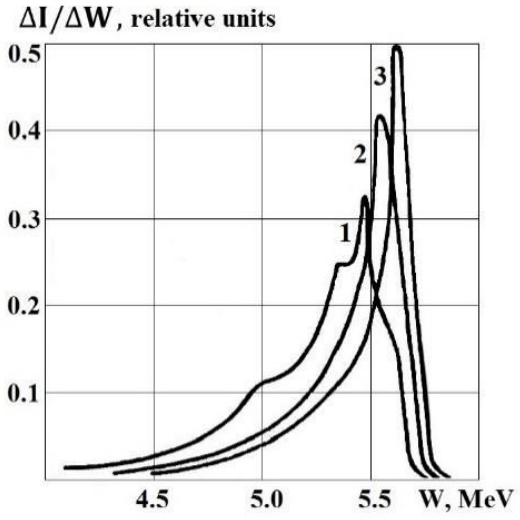

Figure-2. Energy spectrum at the output of two-section accelerator: 1) $-(\tau_p = 3\mu s, \tau_1 = 0)$; 2) $-(\tau_p = 3\mu s, \tau_1 = 1.0\mu s)$; 3) $-(\tau_p = 1.5\mu s, \tau_1 = 1.0\mu s)$.

It was found that at optimum delay of injection pulse the width of distribution function at half-height equals to 4.5%, which is by 1.6 times lower than without delay. At the same time average beam energy slightly increases. The same figure shows spectrum at duration of injection pulse $\tau_p = 1.5\mu s$ and $\tau_1 = 1\mu s$. In this case the scatter due to acceleration of electrons upon drop of HF pulse is excluded and the spectrum width decreases to 3%.

A series of similar measurements at different P_0, I_0 and f_0 demonstrates that the spectrum width instead of $8 \div 23\%$ without delay amounts from 3.5% to 6% with optimum delay. When half duration of injection pulse was used the respective values were as follows: $5 \div 6\%$ without delay and $2 \div 3.5\%$ with optimum delay.

The obtained results demonstrate that the delay of injection pulse in standing wave linac would allow decreasing significantly the energy spectrum width of accelerated electrons to 2%, moreover, technical implementation of the delay is readily available.

However, in this case the electron efficiency of accelerator decreases due to increase in HF energy wastes. Let us consider some standing wave linacs which improve output properties of accelerators with simultaneous increase in their electron efficiency.

According to Eq. (1) energy loss upon transient process equals to $W_{loss} = \frac{P_0 Q_0}{(1+\chi)\omega_0}$.

It can be seen that the loss of high-Q systems is high and substantial at low durations of HF pulse. For the considered class of accelerators the pulse duration is in comparatively narrow range $0.1 \div 5\mu s$, which is determined on the one hand by onset time of oscillations in self-excited generator, and, on the other hand, by sparkling, cathode emission drop, and transition of generation frequency to another type of oscillations [8]. Therefore, energy loss caused by transient process can amount to tens of per cents in standing wave linac.

Figure-3(a) illustrates the flowchart of cascade connection of HF bridges which improves output properties of multi-sectional standing wave linacs with simultaneous increase in electron efficiency of these devices. With this aim the output arms of the first bridge are connected to two grouping sections of separate resonators, and those of the second and subsequent bridges to identical accelerating sections. The second output arm of the last bridge is connected to absorbing HF loading. The coupling coefficient of accelerating and grouping sections with input waveguides is selected on the basis of the following equations:

$$\beta_0 = \frac{2P_g - P_{01} + 2\sqrt{P_g{}^2 - P_{01}}}{P_{01}}, \qquad (3)$$

$$\beta_k = 2(N-k) - 1 + 2\sqrt{(N-k)(N-k-1)},$$

where β_0 is the coupling coefficient of grouping sections with the arms of the first bridge; P_g is the nominal power of HF generator; P_{01} is the nominal active power of grouping sections; β_k is the coupling coefficient of each pair of accelerating sections with the arms of coupled HF bridge; N is the total amount of HF bridges; $k = 1, 2, \ldots N-1$ is the number of pair of accelerating sections connected to one HF bridge.

Generally, bunching system in standing wave linac consumes comparatively moderate portion of energy supplied from HF generator, thus, the main portion of incident wave reflects from it. According to Eq. (3) the coupling coefficient with input waveguide corresponds to the mode of strong over-coupling. Hence, the time of transient process sharply decreases, the time constant of this process is $\tau = \frac{2Q_0}{(1+\beta)\omega_0}$, where $\beta_0 \gg 1$.

In subsequent sections the transient process is accelerated both due to increase in β_k, and due to increasing HF energy supplied the section input in comparison with steady mode as a consequence of reflections from previous sections.

Therefore, even in the last pair of accelerating sections operating in the mode of critical coupling the transient process is slightly accelerated. If HF system of the accelerator is arranged according to such layout, then the transient process in bunching system will be faster by 17 times. This would improve acceleration conditions of electrons at leading edge of HF pulse envelope and enable actually complete elimination of particles previously accelerated at pulse falling edge. As a consequence the width of energy spectrum decreases by $2 \div 3$ times, herewith, HF energy loss in waveguide loading decreases by 30%, that is, accelerated current slightly increases by about 5%. It should be mentioned that in addition the dimensions of HF system becomes more compact due to removal of one absorbing loading from the flowchart.

Figure-3b illustrates the modification of this HF system for three-section accelerator with the following coupling coefficients of resonator sections with input waveguides: $\beta_1 = \beta_2 = 3 + \sqrt{2}$, $\beta_3 = 1$.

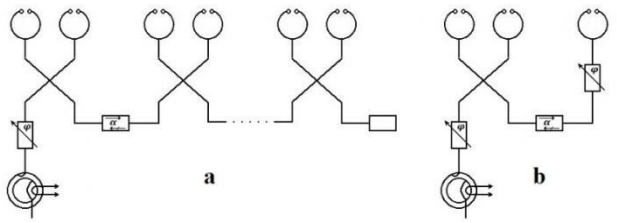

Figure-3. HF supply power system: a) multi-sectional accelerator; b) three- section accelerator.

That is, the first two sections consume by 25% of HF generator energy and the third one consumes 50%. With such configuration well grouped electron clusters with low phase duration are generated at output of the second section. Using phase invertor, modifying entry phase of clusters into the third section, it is possible to fine tune the electron energy at accelerator output. Coupling ratio somewhat differs from $3dB$, which enables stabilization of magnetron frequency using high-Q resonators. Herewith, the third section does not influence on generator operation since it is completely decoupled from generator by ferrite isolator.

It should be mentioned that such systems were considered with assumption of zero current loading. In order to account for the value of accelerated current the coupling coefficients of resonator sections with input waveguides should be adjusted; then, maximum HF energy is supplied to accelerating sections even with non-zero current loading.

3. CONCLUSIONS

In the considered high-frequency systems of linac supply generator was completely decoupled from high-Q accelerating sections is achieved, the influence of current load by accelerating sections decreases, and beam output properties are improved.

These systems permit fine tuning of HF energy supplied to accelerating resonator sections and simultaneous variation of time constant of transient process of electric fields setup in the sections. Addition of facilities for implementation of wide-scale tuning of accelerated beam parameters without impairing of its quality into accelerating and high frequency systems creates conditions for successful solution of wide range of experimental and practical tasks using similar devices. Such universalization would permit to arrange serial production and successful implementation of such accelerators.

We plan to consider designs of coupling cells and input unit of high-frequency power of standing wave linac and HF focusing [9,10], which would permit tuning of accelerating current with optimum mode of electron acceleration and tuning adjustment of beam output energy at fixed value of accelerating current.

ACKNOWLEDGEMENTS

This work was supported by MEPhI Academic Excellence Project (contract No. 02.a03.21.0005, 27.08.2013).

REFERENCES

[1] Lapostolle P. and Septier A. 1970. Linear Accelerators. Amsterdam: North Holland.

[2] Novozhilov et al. 2016. Calculation of Resonant Frequencies and Electromagnetic Fields in Resonators of Linear Accelerators for Commercial Application, Medicine and Environmental Protection. Research Journal of Pharmaceutical, Biological and Chemical Sciences. 7(2): 897-905.

[3] Vikulov V.F., Zavadtsev A.A. and Zverev B.V. et al. 1979. A Compact Standing-Wave Electron Linac with Rf Drive System Using 3 Db Hybrid Junction. IEEE Transactions on Nuclear Science, NS-26(3): 4292-4293.

[4] Novozhilov A.E. et al., 2016. Distribution of Accelerating Voltage in Resonator of Linear Electron-Positron Collider. International Journal of Applied Engineering Research. 11(3): 1596-1602.

[5] Vikulov V.F., Gorbatov V.S. and Rashchikov V.I. 1979. Energy Spectrum of Resonator Electron Accelerator. In: Accelerators (Issue 17). Moscow: Atomizdat. pp. 21-26.

[6] Zavorotylo V.N. 1979. Excitation of high frequency oscillations in linear standing wave electron accelerators. Candidate Thesis. National Research Nuclear University (MEPhI), Moscow.

[7] Val`dner O.A., Vlasov A.D. and Shal`nov A.V. 1969. Linear Accelerators. Moscow: Atomizdat.

[8] Lebedev I. V. 1972. Microwave Technology and Instruments (Vol. 2). Moscow: Vysshaya Shkola.

[9] Filatov, A.N. and Shilov, V.K. 1984. RF Focusing in the Standing-Wave Electron Linacs. Soviet physics. Technical physics. 29(2): 163-167.

[10]Filatov, A.N., and Shilov, V.K. 1985 Control of radio-frequency characteristics of linear electron accelerator. Instruments and Experimental Techniques New York. 28(6 pt 1): 1258-1261.